Damping of Sloshing in a Moving Container

Sherif Amer[1], Peter Zentgraf[1], Eduard Ober[1]

Abstract

Liquid sloshing limits speed, accuracy, and reliability of pick-and-place systems, laboratory automation, and mobile robots that transport open containers. Motivated by industrial anti-sloshing motion functions [1], this work presents a compact testbed and a simple open-loop strategy that reproduces the effect on a low-cost setup. A camera rigidly mounted to the carriage moves with the tank and records the free surface, enabling extraction of the visible surface angle per frame. The first two sloshing frequencies and the dominant-mode damping are identified from experiments. The dominant mode is then modeled as a lightly damped second-order system excited by the carriage motion. Two command-side strategies are compared: Zero-Vibration-Derivative (ZVD) input shaping and an inverse transfer function prefilter. The ZVD method delivers near-zero residual slosh after the end of the move with a predictable, fixed time extension equal to the damped period. The inverse function prefilter also suppresses the sloshing with the advantage of being a simpler approach. Both approaches are open-loop and need only the identified frequency and damping for a given fill level of the container. A single-mode simulation based on the identified model predicts the measured behaviour successfully, and both suppression strategies are verified in simulation and experiments.

Keywords

Sloshing, input shaping, system identification, feedforward control, vibration suppression

1 Introduction

Sloshing in moving containers is a pervasive problem in engineering sectors ranging from automotive and aerospace to food processing and laboratory automation. When a container is accelerated, the free surface of the liquid deviates from its equilibrium, resulting in standing waves. In industrial packaging and transport, these oscillations can lead to spillage, container instability due to shifting center of mass, and the introduction of air bubbles into viscous fluids. To maintain process integrity, manufacturers are often forced to limit the acceleration and velocity of their transport systems, directly reducing production throughput.

Control strategies for sloshing suppression fall into two categories: feedback (closed-loop) and feedforward (open-loop). Feedback control requires real-time measurement of the fluid state, typically using wave probes, capacitive sensors, or force/torque sensors. While effective, these sensors are often intrusive, expensive, or impractical for high-speed conveyor belts. Consequently, open-loop strategies have gained prominence. These methods modify the motion command sent to the actuator to avoid exciting the system's natural frequencies.

The most established open-loop technique is Input Shaping, pioneered by Singer and Seering [2]. By convolving the command signal with a sequence of impulses, the vibration induced by the first impulse is cancelled by subsequent impulses. This work presents a complete workflow: from the con-

[1] Technische Hochschule Rosenheim

Open Access. © 2026 Sherif Amer, Peter Zentgraf, Eduard Ober
This work is licensed under the Creative Commons Attribution 4.0 License. +

struction of a low-cost testbed and the identification of a high-fidelity plant model, to the rigorous comparison of filtering, shaping, and inverse dynamic methods.

2 Experimental System

The motion platform is based on a Linseis LY 1900 PL XY-plotter, retrofitted to operate as a single-axis linear stage. The original control electronics were bypassed in favour of a modern microcontroller interface. An Arduino MKR Zero serves as the real-time control unit. It receives digital position setpoints via USB serial communication and converts them into analogue voltage signals using an Adafruit AD5693 16-bit Digital-to-Analog Converter (DAC). This high-resolution analogue signal drives the plotter's internal servo loop, ensuring smooth motion.

A rectangular acrylic container ($100 \times 100 \times 50$ mm) is mounted to the carriage, as shown in Figure 1. To monitor the system state, an LSM303D 3-axis accelerometer is attached to the carriage, communicating with the Arduino via I^2C. Additionally, the plotter's internal optical encoders provide position feedback, which is logged to verify that the carriage accurately follows the shaped commands.

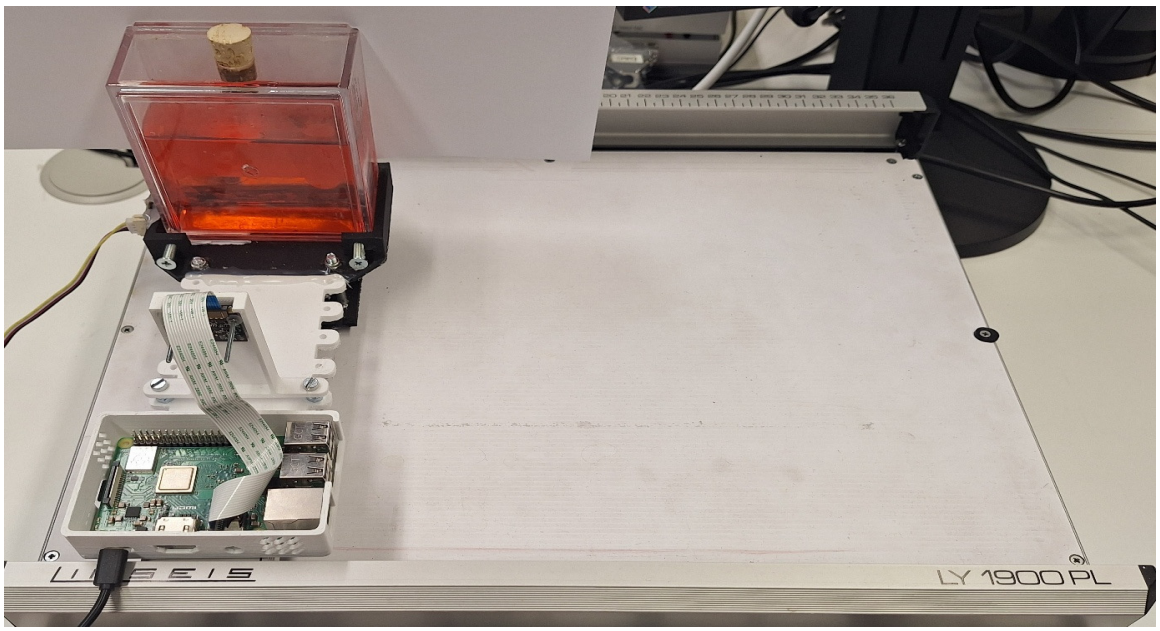

Figure 1: The Experimental Testbed. The Linseis LY 1900 PL plotter with the transparent container, Raspberry Pi camera system, and control electronics mounted on the moving carriage.

3 System Modelling and Identification

Effective open-loop control requires an accurate mathematical model of the system. This section describes the theoretical structure of the slosh dynamics and details the experimental identification process.

Open Access. © 2026 Sherif Amer, Peter Zentgraf, Eduard Ober
This work is licensed under the Creative Commons Attribution 4.0 License. +

3.1 Theoretical Hydrodynamics

The dynamics of general sloshing are governed by the Navier-Stokes equations, but for rigid containers undergoing linear motion, the behaviour is dominated by distinct resonant modes. These are categorized as symmetric and antisymmetric modes. Symmetric modes do not generate lateral forces and are generally negligible for translational motion. Antisymmetric modes, however, involve the lateral displacement of the liquid's center of mass and are the primary concern for motion control.

For a rectangular tank of length L filled to a depth h, linear wave theory predicts that the natural frequency ω_n of the n-th antisymmetric sloshing mode is given by the dispersion relation [3].

$$\omega_n = \sqrt{g k_n \tanh(k_n h)} \#(1)$$

where g is the gravitational acceleration and k_n is the wave number, defined as:

$$k_n = \frac{(2n-1)\pi}{L} \#(2)$$

For the experimental setup ($L = 0.1\,m$, $h = 0.061\,m$), the fundamental mode ($n = 1$) is calculated as:

$$\omega_1 = \sqrt{9.81 \left(\frac{\pi}{0.1}\right) \tanh\left(\frac{\pi}{0.1} \times 0.061\right)} \approx 17.19 \text{ rad/s}$$

$$\omega_2 = \sqrt{9.81 \left(\frac{3\pi}{0.1}\right) \tanh\left(\frac{3\pi}{0.1} \times 0.061\right)} \approx 30.41 \text{ rad/s}$$

This corresponds to a frequency of $f_1 \approx 2.74\,Hz$. The second antisymmetric mode (n=2) is predicted at $f_2 \approx 4.84\,Hz$. These theoretical values provide a baseline for experimental identification.

3.2 Experimental Identification

To easily integrate the sloshing dynamics into a control framework, the sloshing liquid is modelled as a mechanical pendulum. The dynamics of the dominant slosh mode are approximated as a linear time-invariant (LTI) second-order system. Since the fluid motion is driven by the acceleration of the tank, the transfer function from carriage position $U(s)$ to slosh angle $\Theta(s)$ takes the form:

$$G(s) = \frac{\Theta(s)}{U(s)} = \frac{K s^2}{s^2 + 2\zeta\omega_n s + \omega_n^2} \#(3)$$

To obtain the second-order transfer function, the ‘pzMove’ system identification tool was employed [4], [5]. This tool utilizes a numerical optimization algorithm to minimize the least-squares error between the measured output and the simulated response of the model structure. The input for the identification process was the commanded position profile of a simple ramp of the carriage $u(t)$, and the output was the corresponding measured free-surface angle $\theta(t)$, obtained from the vision system during the move at a fill level of 6.1 cm.

The resulting identified model is:

$$G_{id}(s) = \frac{-26.216 s^2}{s^2 + 0.703 s + 317.14} \#(4)$$

The resulting identification, shown in Figure 2, demonstrates a high-quality fit between the measured data (red line) and the simulated response of the identified model (green dashed line).

Open Access. © 2026 Sherif Amer, Peter Zentgraf, Eduard Ober
This work is licensed under the Creative Commons Attribution 4.0 License. +

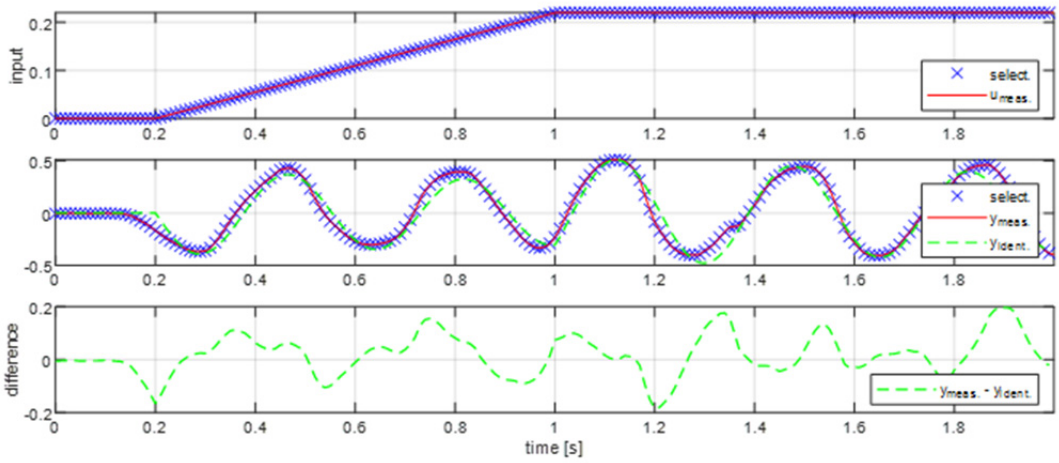

Figure 2: Comparison of simulated and measured signals in pzMove.

4 Sloshing Suppression Methods

Two open-loop control strategies were designed based on the identified model and sloshing frequencies.

4.1 Input Shaping

Input shaping is a classical and highly effective feedforward control technique that convolves the original, unshaped command with a precisely timed sequence of impulses. The fundamental concept is to generate a series of self-canceling oscillations. The first impulse in the sequence initiates a motion and, consequently, a sloshing wave. Subsequent impulses are timed to arrive at specific fractions of the slosh period, initiating new waves that are perfectly out of phase with the original wave, thereby destructively interfering with it and canceling it out.

The amount of residual vibration V, resulting from a sequence of n impulses can be expressed as a function of the system's frequency ω and damping ζ [2]:

$$V(\omega,\zeta) = e^{-\zeta\omega t_n}\sqrt{\left(\sum_{i=1}^{n} A_i e^{\zeta\omega t_i}\cos\left(\omega\sqrt{1-\zeta^2}\,t_i\right)\right)^2 + \left(\sum_{i=1}^{n} A_i e^{\zeta\omega t_i}\sin\left(\omega\sqrt{1-\zeta^2}t_i\right)\right)^2} \#(5)$$

where A_i and t_i are the amplitudes and time locations of the impulses, and ω_d is the damped natural frequency. To achieve zero vibration, the terms inside both parentheses must be driven to zero.

4.1.1 ZV Shaper

The simplest input shaper is the Zero Vibration (ZV) shaper, which uses two impulses. To ensure the impulses are properly scaled and non-trivial, a constraint is imposed that their amplitudes must sum to one: $\sum A_i = 1$. For zero residual vibration, the sine and cosine terms in the equation for $V(\omega,\zeta)$ must both be zero. For a two-impulse sequence starting at $t_1 = 0$, this requires:

$$A_2 e^{\zeta\omega t_2}\sin(\omega_d t_2) = 0 \#(6)$$

$$A_1 + A_2 e^{\zeta\omega t_2}\cos(\omega_d t_2) = 0 \#(7)$$

Open Access. © 2026 Sherif Amer, Peter Zentgraf, Eduard Ober
This work is licensed under the Creative Commons Attribution 4.0 License. +

The first equation is satisfied when the sine term is zero, which occurs when the second impulse is timed at a multiple of the half-period of the damped oscillation. The shortest possible delay time (for the fastest response) is half a period: $t_2 = \pi/\omega_d = T_d/2$.

With this timing, and by solving the second equation simultaneously with the amplitude constraint ($A_1 + A_2 = 1$), the amplitudes are found to be:

$$A_1 = \frac{1}{1+K}, \quad A_2 = \frac{K}{1+K} \quad \text{where} \quad K = e^{-\zeta\pi/\sqrt{1-\zeta^2}} \#(8)$$

This two-impulse ZV shaper will theoretically produce zero vibration after the second impulse, but in real-world applications this is not the case as it would require perfect knowledge of the system's parameters. The primary drawback of the ZV shaper is its high sensitivity to modeling errors. If the actual natural frequency of the system differs slightly from the frequency used to design the shaper, significant vibration can still occur.

4.1.2 ZVD Shaper

To overcome this limitation, more robust shapers are designed by imposing additional constraints. The Zero Vibration Derivative (ZVD) shaper adds the constraint that the derivative of the residual vibration with respect to frequency must also be zero at the design frequency [2]:

$$\frac{d}{d\omega} V(\omega, \zeta) = 0 \#(9)$$

This creates a shaper that is much more tolerant of frequency modeling errors. Small deviations from the nominal frequency still result in low residual vibration. Satisfying this additional constraint requires a third impulse. The resulting three-impulse ZVD shaper, which was chosen for this project, has impulse timings at $t = [0, 0.5T_d, T_d]$. The amplitudes are also calculated from the system's frequency and damping to satisfy all three constraints (zero vibration, zero derivative, and sum of amplitudes equals one).

$$A_1 = \frac{1}{1+2K+K^2}, \; A_2 = \frac{2K}{1+2K+K^2}, \; A_3 = \frac{K^2}{1+2K+K^2} \#(10)$$

The experimental identification revealed a dominant slosh mode at $f_1 = 2.8$ Hz and a secondary mode at $f_2 = 5.2$ Hz. To ensure robust performance, a two-mode ZVD shaper was designed to simultaneously cancel oscillations at both frequencies. This is achieved by mathematically convolving both the three-impulse ZVD sequence designed for f_1 and the three-impulse ZVD sequence designed for f_2 with the original position command. The resulting position command is capable of suppressing both modes.

The primary advantage of ZVD is increased robustness to modeling errors. The main trade-off is that it introduces a time delay equal to T_d (the time of the last impulse) compared to $\frac{1}{2}T_d$ for ZV, meaning the ZVD shaped motion profile will take longer to complete.

4.2 Inverse Transfer Function Prefilter

An alternative feedforward strategy is to directly invert the dynamics of the system. The goal of this method is to design a pre-filter, $F(s)$, that, when placed in series with the plant model $G(s)$, results in an overall transfer function of unity. If this is achieved, the output of the system will perfectly track the desired trajectory. The identified transfer function from position command $U(s)$ to surface angle $\Theta(s)$ is:

$$G_{u\to\theta}(s) = \frac{\Theta(s)}{U(s)} = \frac{-26.216\, s^2}{s^2 + 0.70305\, s + 317.14} \#(11)$$

Open Access. © 2026 Sherif Amer, Peter Zentgraf, Eduard Ober
This work is licensed under the Creative Commons Attribution 4.0 License. +

The objective is to find a pre-filter $F(s)$ that computes the necessary position command $U(s)$ from a desired surface angle trajectory $\Theta_d(s)$. The ideal pre-filter to cancel out the oscillations is of course the mathematical inverse of the plant model:

$$F(s) = G^{-1}(s) = -\frac{1}{26.216}\frac{s^2 + 0.70305s + 317.14}{s^2} \#(12)$$

By separating the terms of the inverse transfer function, we can express the relationship in the frequency domain as:

$$U(s) = -\frac{1}{26.216}\left(1 + \frac{0.70305}{s} + \frac{317.14}{s^2}\right)\Theta_d(s) \#(13)$$

Applying the Inverse Laplace Transform yields the control law for the carriage position $u(t)$:

$$u(t) = -\frac{1}{26.216}\left[\theta_d(t) + 0.70305\int_0^t \theta_d(\tau)d\tau + 317.14\iint_0^t \theta_d(\tau)d\tau^2\right] \#(14)$$

To ensure smooth motion with zero residual oscillation, the desired angle trajectory $\theta_d(t)$ is chosen as a single period of a sine wave with duration T_{move}.

$$\theta_d(t) = A\sin\left(\frac{2\pi}{T_{move}}t\right), \quad 0 \le t \le T_{move} \#(15)$$

The amplitude A determines the total distance travelled. At the end of the move ($t = T_{move}$), the angle θ_d and its first integral are zero for a full sine period. Thus, the final position X_{final} is determined solely by the double integral term:

$$\iint_0^{T_{move}} \theta_d(\tau)d\tau^2 = \int_0^{T_{move}} \frac{A}{\omega_m}(1 - \cos(\omega_m t))\mathrm{dt} = \frac{A}{\omega_m}\left[t - \frac{1}{\omega_m}\sin(\omega_m t)\right]_0^{T_{move}} = \frac{AT_{move}^2}{2\pi} \#(16)$$

$$\mathrm{A} = \frac{(2\pi)(-26.216)X_{final}}{317.14T_{move}^2} = \frac{2\pi \mathrm{K} X_{final}}{\omega_n^2\ T_{move}^2} \#(17)$$

5 Simulation Results

To validate the control strategies before physical implementation, the identified plant model $G_{id}(s)$ was used to simulate the system response. The simulation evaluates the effectiveness of the feedforward controllers in an ideal environment where the model parameters match the system perfectly.

Regarding the inverse prefilter strategy, the analytical approach ensures that the generated position command $u(t)$ moves the carriage exactly X_{final} meters while inducing a fluid response that perfectly tracks the sine profile. The resulting ideal profile is shown in Figure 3.

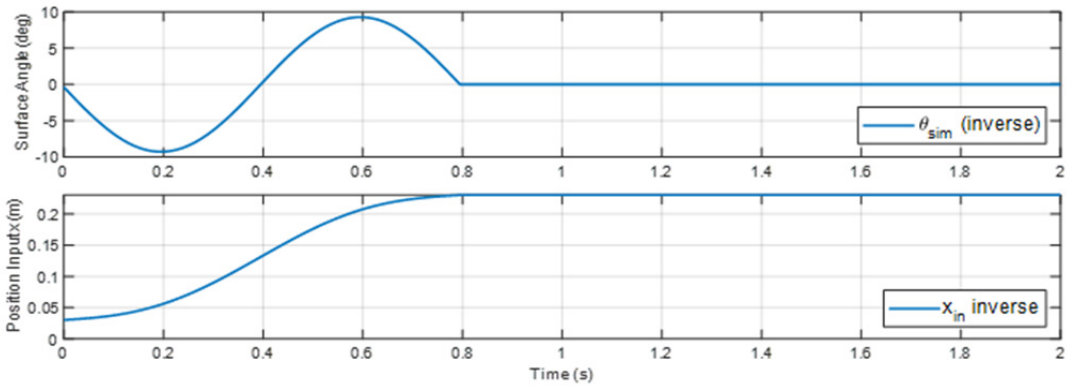

Figure 3: The top plot displays the desired sinusoidal trajectory for the surface angle, and the bottom plot shows the calculated position command required to generate this specific fluid response.

Open Access. © 2026 Sherif Amer, Peter Zentgraf, Eduard Ober
This work is licensed under the Creative Commons Attribution 4.0 License.

Figure 4 compares the system response to a standard unshaped ramp command versus a Zero Vibration (ZV) shaped command. The unshaped input excites the system's natural frequency. The ZV shaper, designed for the dominant identified frequency, modifies the input steps to cancel the vibration. The simulation shows that the ZV shaper significantly reduces the oscillation amplitude during and after the move, confirming the theoretical cancellation of the dominant mode.

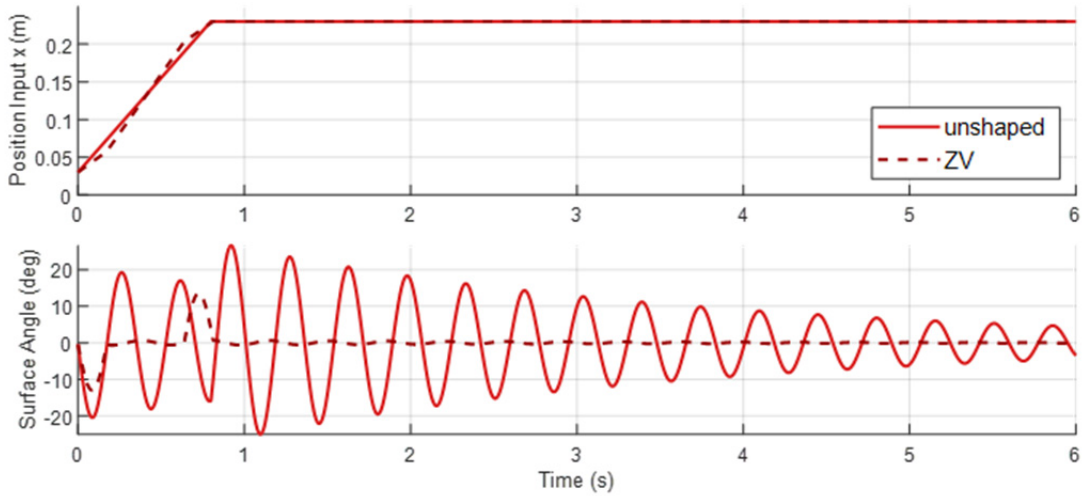

Figure 4: Simulation results comparing the system response to a standard unshaped ramp command versus a Zero Vibration (ZV) shaped command

To further evaluate the proposed methods, a comparative simulation of the ZV shaper, ZVD shaper, and Inverse Transfer Function prefilter was conducted, as shown in Figure 5.

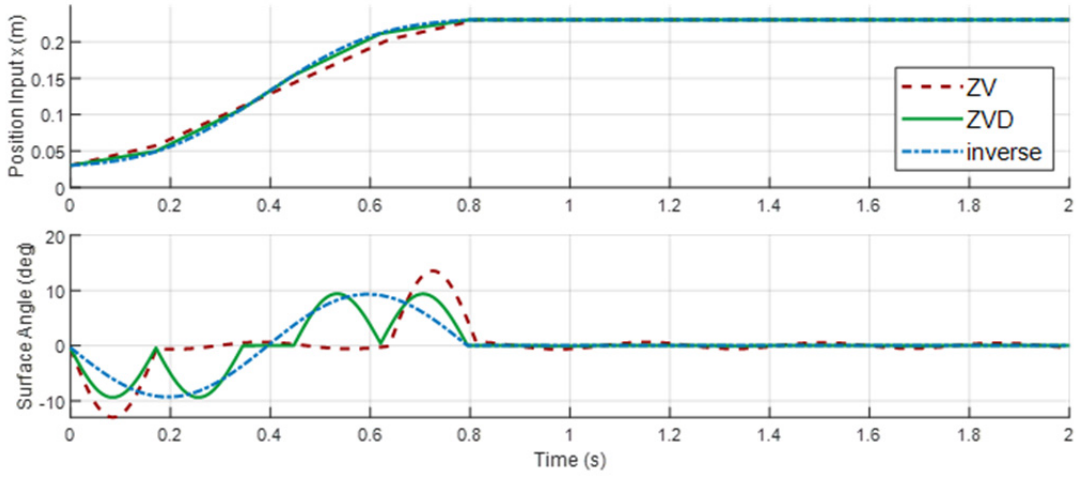

Figure 5: Comparative simulation of the suppression strategies. The plots display the position inputs (top) and resulting surface angles (bottom) for the ZV shaper, ZVD shaper, and Inverse Prefilter.

6 Experimental Results

This chapter presents the experimental results and analysis for the sloshing suppression methods designed in this project. The performance of the various input shapers and the inverse prefilter is systematically evaluated on the physical testbed. To ensure a fair comparison, the motion profiles are designed to have a total move time equal to each other.

Open Access. © 2026 Sherif Amer, Peter Zentgraf, Eduard Ober
This work is licensed under the Creative Commons Attribution 4.0 License. +

6.1 Input Shaping

First, a baseline move using an unshaped ramp profile was executed. As seen in the results, this induced significant sloshing with a peak amplitude of approximately 24 degrees, which persisted with very little natural damping long after the move was completed.

The implementation of the Zero Vibration (ZV) shaper (Figure 6) significantly reduced the initial transient spike. However, due to the high sensitivity of the ZV shaper to modeling errors and the presence of the secondary sloshing mode, noticeable residual vibration remained after the move with a maximum of about 14 degrees.

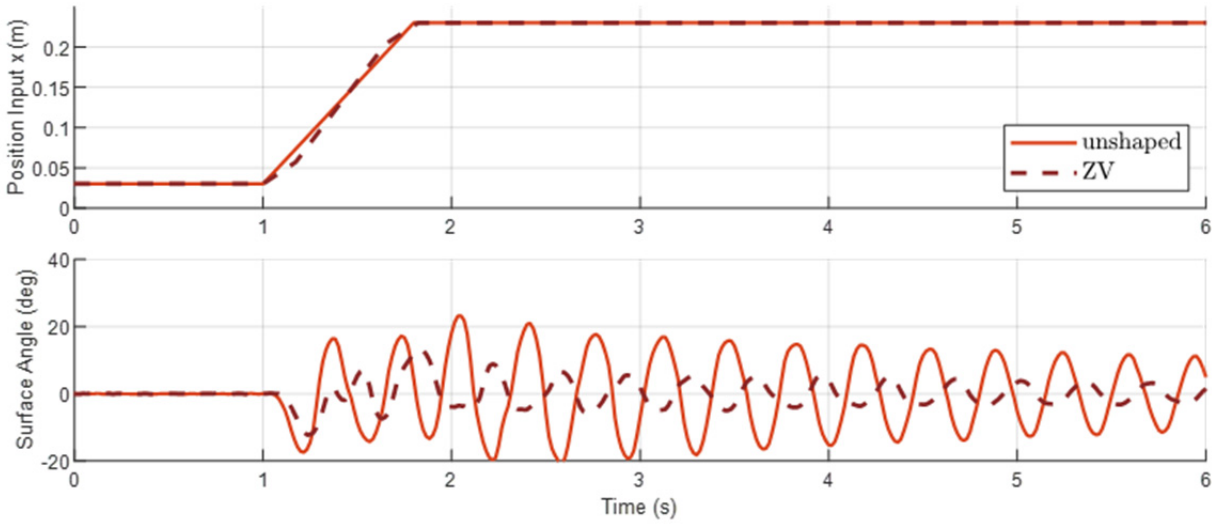

Figure 6: Experimental comparison of the ZV shaper against a baseline unshaped move.

To improve performance, the Zero Vibration Derivative (ZVD) shaper was applied. In figure 7 the unshaped move is compared against a 1-mode ZVD shaper designed for the dominant frequency.

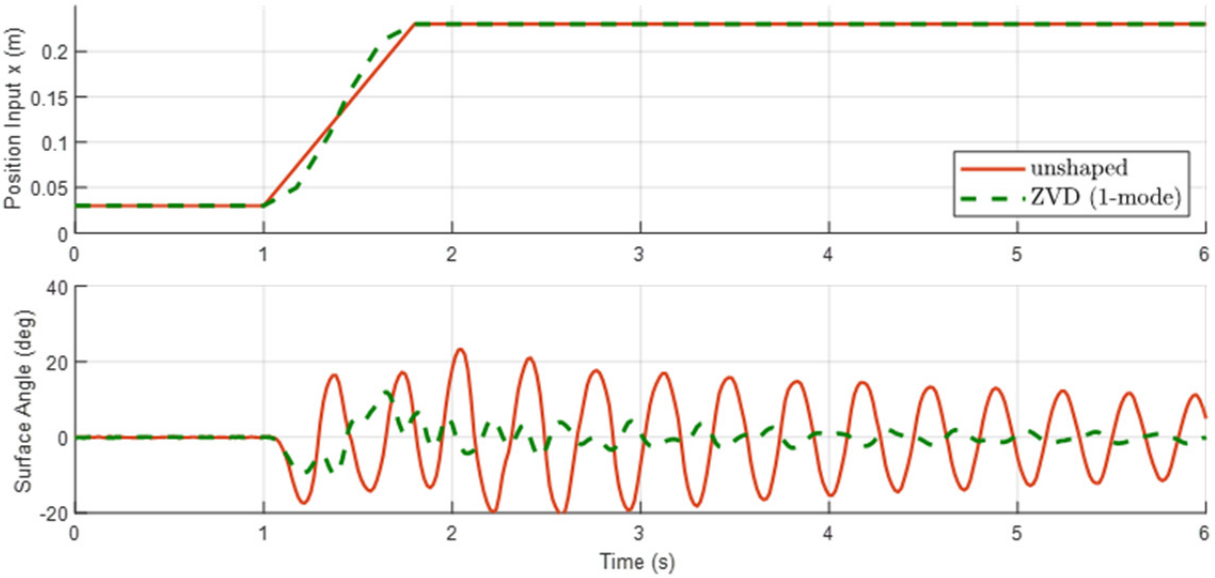

Figure 7: Experimental comparison of the ZVD shaper against a baseline unshaped move.

Open Access. © 2026 Sherif Amer, Peter Zentgraf, Eduard Ober
This work is licensed under the Creative Commons Attribution 4.0 License. +

Figure 8 demonstrates the effectiveness of the 2-mode ZVD shaper, designed to suppress both f_1 and f_2. By convolving the shapers for both frequencies, the residual vibration is virtually eliminated, reducing the fluid motion to the noise floor of the sensor immediately upon the completion of the move. The trade-off, however, is an increase in the move duration due to the length of the impulse sequence.

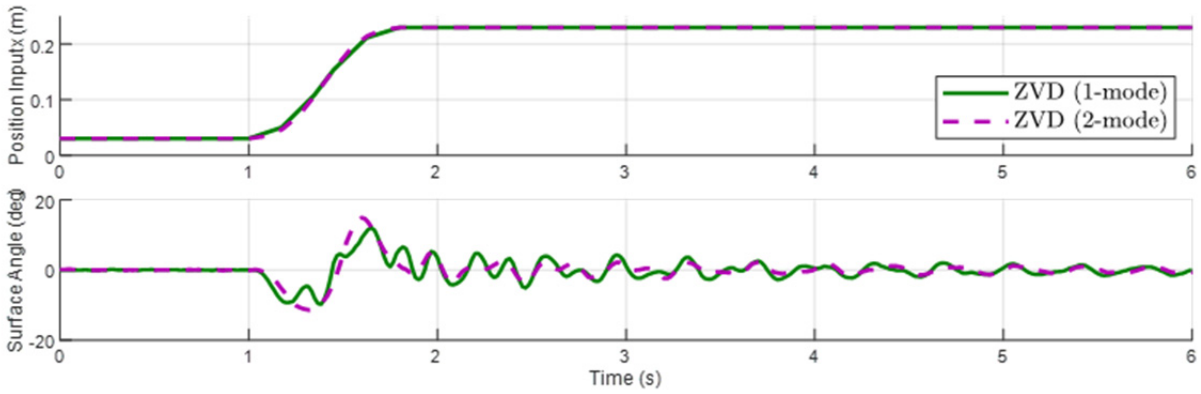

Figure 8: Experimental comparison of the ZVD for the first mode and ZVD for both sloshing modes.

6.2 Inverse Transfer Function Prefilter

The performance of the Inverse Transfer Function strategy is analysed in figure 9. The goal was to force the fluid surface to track a specific trajectory, a single period of a sine wave rather than simply suppressing vibration at the end of the move.

The results show the measured surface angle compared to the unshaped response and the theoretical reference. The blue dashed line represents the inverse solution designed for the sinusoidal angle trajectory. The experimental data shows remarkable agreement with the theoretical design; the fluid angle rises and falls following the sine profile and settles immediately to zero shortly after the carriage comes to a halt.

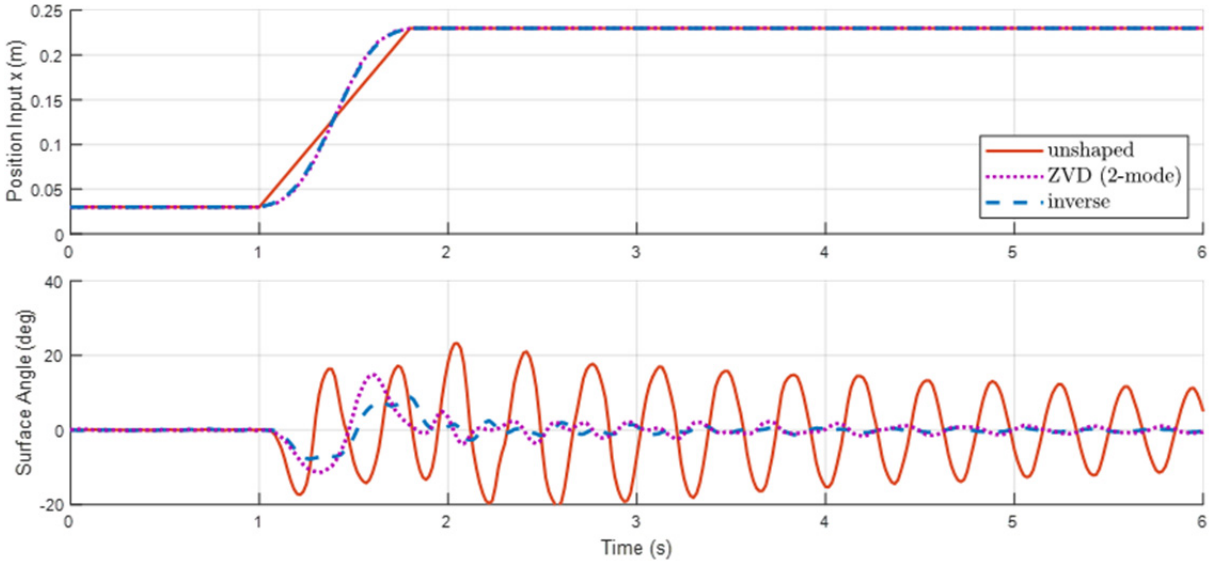

Figure 9: Performance comparison between the inverse prefilter and the two-mode ZVD shaper.

Open Access. © 2026 Sherif Amer, Peter Zentgraf, Eduard Ober
This work is licensed under the Creative Commons Attribution 4.0 License. +

It is important to note that no deep theoretical knowledge is necessary to design an effective profile to reduce the liquid sloshing. Basic knowledge of one semester in feedback control is sufficient to use the inverse prefilter method.

7 Conclusion

This work successfully validated a low-cost, open-loop framework for eliminating liquid sloshing using a retrofitted testbed and vision-based system identification. By deriving an accurate second-order model, the study demonstrated that effective damping is achievable without the need for complex feedback sensors or physical baffles. The experimental results highlighted a distinct trade-off between the two primary control strategies: while the two-mode Zero Vibration Derivative (ZVD) shaper offered robustness by canceling both dominant and secondary frequencies, it introduced a predictable time delay that extended the move duration. In contrast, the Inverse Transfer Function prefilter proved highly efficient, forcing the fluid dynamics to strictly conform to a sinusoidal trajectory and achieving zero residual sloshing without the time penalties associated with multi-mode shaping.

These findings suggest that if the system model is sufficiently accurate, inverse dynamic methods can offer superior throughput for industrial pick-and-place applications compared to traditional input shaping. The ability to reduce fluid motion to the noise floor of the sensor validates the effectiveness of the identified plant model. Future work is proposed to address the sensitivity of these open-loop methods by exploring more robust techniques, such as Extra-Insensitive (EI) shapers, to better handle parameter uncertainty. Additionally, the framework will be tested against varying fill levels and complex container geometries to further verify its versatility in diverse manufacturing environments.

8 References

[1] B&R Industrial Automation, “Boost productivity with anti-sloshing,” Press Room, Aug. 6, 2017. Accessed Sep. 24, 2025.

[2] Singer, N. C., Seering, W. P., Preshaping command inputs to reduce system vibration, ASME Journal of Dynamic Systems, Measurement, and Control, 1990, 112(1), 76-82.

[3] F. T. Dodge, The New "Dynamic Behavior of Liquids in Moving Containers". San Antonio, TX: Southwest Research Institute, 2000.

[4] P. Zentgraf. Ein neues Verfahren zur Modellierung linearer Systeme – Experimentelle Modellbildung mit Ein- und Ausgangsdaten. atp magazin, 2019.

[5] pzMove, Learning-Tool of the Control engineering laboratory, https://www.th-rosenheim.de/die-hochschule/labore/regelungstechnik/pzmove, University of applied science Rosenheim.

[6] S. Amer, “Modelling and damping of sloshing in a moving container,” Master's project, Technische Hochschule Rosenheim, Rosenheim, Germany, 2026. Accessed at https://www.th-rosenheim.de/fileadmin/fakultaeten/ing/Bilder/02_Labore/Mess-_und_Regelungstechnik/Ingenieurprojekte/Modelling_and_Damping_of_Sloshing_in_a_Moving_Container/Sloshing_Report_Sherif_Amer.pdf

Open Access. © 2026 Sherif Amer, Peter Zentgraf, Eduard Ober
This work is licensed under the Creative Commons Attribution 4.0 License. +